Cold Regions Science and Technology 98 (2014) 26–34

Contents lists available at ScienceDirect

Cold Regions Science and Technology

journal homepage: www.elsevier.com/locate/coldregions

Mechanical properties of a silty clay subjected to freezing–thawing

Zhen-Dong Cui *, Peng-Peng He, Wei-Hao Yang

State Key Laboratory for Geomechanics and Deep Underground Engineering, School of Mechanics and Civil Engineering, China University of Mining and Technology, Xuzhou, Jiangsu 221116, PR China

ARTICLE INFO

Article history:
Received 7 August 2013
Accepted 26 October 2013

Keywords:
Freezing and thawing
Laboratory test
Constitutive relationship
Silty clay
Microstructure

ABSTRACT

The structure of soil will change a lot after freezing and thawing. The mechanical properties and the microstructures are quite different from those of the undisturbed soil. Based on the static triaxial tests and dynamic triaxial tests, this paper studied the mechanical characteristics of a silty clay and quantitatively analyzed the scanning electron microscopy (SEM) images of the silty clay before and after freezing and thawing. According to the static triaxial test and the disturbed state concept (DSC), the constitutive relationship of the thawing soil was investigated. The dynamic triaxial tests were conducted to study the dynamic constitutive relationship of the thawing soil and the mechanical parameters were compared with those of the undisturbed soil. The parameters of the microstructures of silty clay were extracted to analyze the influences of the freezing and thawing on silty soil.

1. Introduction

With the large-scale exploitation of underground space, freezing method has been widely used for tunneling in the soft soil area, especially in soil body reinforce of tunnel by-pass and underground pumping room, etc. But it had ever caused serious geological hazard and deformation or leakage around tunnel after operation. Thus it is important to understand how to use freezing method for tunneling safely, economically and reasonably in engineering construction. In addition, after the excavation of tunnel, a plenty of frozen soil, which will melt and result in the deformation of tunnel, remains around tunnel.

There are two major problems for the soil after freezing and thawing. The one is the action of freezing and thawing and the other is the effect of cyclic dynamic loads. For the former, the internal structures and the joint forces of undisturbed soil were destroyed during the period of freezing and thawing (Graham and Au, 1985; Konrad, 1989), and thus the action of freezing and thawing has great influence on the physical properties and mechanical features of soil, such as hydraulic permeability, unfrozen water content, strength, compressibility, and bearing capacity (Leroueil et al., 1991; Liu and Peng, 2009; Mahmoud and Mahya, 2013; Qi et al., 2006, 2008). Because of many factors which affect the nature of the thawing in the tests (e.g. the test conditions and the initial state of thawing soil), the understandings of the actual nature of thawing soil were not the same. After freezing and thawing, the changes of elastic modulus (Elliott and Thornton, 1988; Simonsen and Isacsson, 2001; Simonsen et al., 2002) and shear strength (Bondarenko and Sadovsky, 1991; Brams and Yao, 1964; Ono and Mitachi, 1997; Yong et al., 1985) were not exactly identical. The changes of them are related to the soil types (Simonsen et al., 2002) and the freeze–thaw conditions (Li et al., 2013), for example after freezing and thawing, loose soils tend to be densified and dense soils may become looser. Moreover, both loose and dense soils may attain the same void ratio (Konrad, 1989). The main reason is that part of the water in the soil will be frozen to ice in the period of freezing; the volume increment caused by the ice will have a significant effect on the surrounding soil structure. Therefore, for clay and silt with smaller pores, the action of ice will greatly disrupt the structure of soil particle and make soil loose; while for sand with larger pore diameters, the action has little effect on it.

For the latter, the frequency (Ling et al., 2013), vibration number and amplitude (Inozemtsev, 1986) of dynamic loads, and confining pressure (Simonsen and Isacsson, 2001) can affect the changes of soil properties. The soil may exhibit pronounced nonliner and hysteretic behavior under dynamic loads (Lai et al., 2000; Ling et al., 2009, 2013). Although the residual strain induced by repeated cyclic loading is slight and it can be ignored, the residual strain induced by accumulative effect under long-term repeated cyclic loading should not be ignored (Li et al., 2013). Also, the dynamic creep properties of soil under dynamic load will significantly influence the failure strain (Lai et al., 2013). Lai et al. (1999) has made the nonlinear analysis of the tunnel for the coupled problem of temperature and seepage fields in cold regions. Lai et al. (2000) also has derived the mathematical mechanical model and the governing differential equations of the coupled problem of temperature, seepage, and stress fields, to determine the initial stresses of tunnels in cold regions. The soil after the artificial freezing has to withstand the two effects simultaneously. Therefore, in order to study the influence of the two effects on soil, static triaxial and dynamic triaxial tests were carried out for a freezing–thawing silty clay.

* Corresponding author. Tel./fax: +86 516 83995678.
E-mail address: czdjiaozuo@163.com (Z.-D. Cui).

0165-232X/$ – see front matter © 2013 Elsevier B.V. All rights reserved.
http://dx.doi.org/10.1016/j.coldregions.2013.10.009

Studies on the soil properties can be conducted from both the macroscopical phenomenon and the microcosmic mechanism. The changes of soil macroscopic properties are the direct results of the changes of microstructure, and the engineering characteristics of soils are controlled by the state of pore structure of soils to a great extent. Therefore, many macroscopic properties of soil can be explained by its microstructure. Currently, scanning electron microscopy (SEM) has become a common method to analyze the microstructure of soil. Delage et al. (1996) compressed clay samples with different water contents, and explained the change of permeability according to the amount of clay particles. Pusch and Schomburg (1999) had investigated the inapplicability of correlations between macro parameters and permeability coefficient, compressibility. Cui and Tang (2011) studied the microstructure of different soil layers in the region owning high-rise buildings by SEM and the mercury intrusion porosimetry test (MIP). SEM has not only applied on ordinary soil but also on improved soil. Murat (2013) studied the effect of the additives on clays under freeze–thaw conditions. Zhang and Feng (1993) analyzed the attenuation mechanism of cement-modified loess after subjection to freeze–thaw cycles by means of SEM photographs.

In this paper, the static triaxial and dynamic triaxial tests were carried out for a freezing–thawing silty clay. The stress–strain relationship and the pore water pressure–strain relationship were studied, and the influences of the freezing and thawing action on the engineering properties and the effect of cyclic dynamic loads were explored. Based on the disturbed state concept (DSC), the stress–strain relationship under dynamic loads with different frequencies obtained by fitting the test data was studied. The changes of soil properties before and after freezing and thawing under dynamic loads were comparatively analyzed. The microscopic parameters were extracted from SEM images, and the effect of the freezing and thawing on soil microstructures was studied by processing the SEM images before and after freezing and thawing.

2. Sample preparation and test scheme

The undisturbed soil samples were frozen for 12 h in the freezing chamber, and the freezing temperature of the samples was −20 °C. Then the frozen soil samples were sealed in a plastic bag and conservated for 72 h in the water of room temperature. After fully thawing, the soil samples were processed into 80 mm in height, 39.1 mm in diameter by soil cutter. Then, the samples were placed in the saturator for above 24 h. The filter papers 10 mm in width, 60 mm in length were affixed around the samples, to ensure good drainage in the process of consolidation. Finally, the soil samples were consolidated under equipressure consolidation condition.

The static triaxial test was conducted using the scheme of consolidated undrained. Different confining pressures were employed to 6 samples, namely, 100 kPa, 150 kPa, 200 kPa, 250 kPa, 300 kPa and 350 kPa, respectively.

The dynamic triaxial test was conducted by American C.K.C dynamic triaxial apparatus. Its frequency range is 0–2 Hz. The range of confining pressure is 0–1.2 MPa. The maximum exciting force can reach 2500 kN. The dynamic wave in the experiment can be sine wave, rectangular wave, or triangular wave. In the test, the exciting force was sine wave and the frequencies of exciting force applied to the test were 1.0 Hz, 1.5 Hz, and 2.0 Hz, respectively, with the confining pressure of 220 kPa. Each level of vibration loads were carried out for 5 cycles, to obtain the averages of dynamic stress and dynamic strain.

3. Data analysis of static triaxial test

Fig. 1 illustrates variations of stress with strain of the thawing soil under different confining pressures, namely, 100 kPa, 150 kPa, 200 kPa, 250 kPa, 300 kPa and 350 kPa, respectively. The dynamic stress has been found to increase with an increase in the dynamic strain. It has been noted that the tangent modulus decreases continuously with

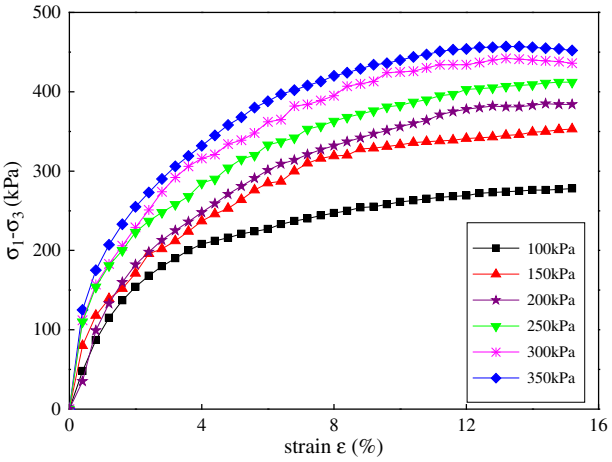

Fig. 1. Variations of Stress with strain.

an increase in the dynamic strain. Then the soil is destroyed gradually. The strain increases sharply, and the stress tends to be constant. The curve is fitting for hyperbola curve. Comparing the 6 curves, it is readily apparent that the peak strength and the initial tangent modulus both increase with an increase in the confining pressure.

Fig. 2 presents the variations of pore water pressure with dynamic strain under different confining pressures. In the beginning, the pore water pressure increases rapidly, then it increases slowly and tends to be stable with the increasing of strain. The trend of pore water pressure–strain curve is the same as the stress–strain curve, the stable value and the initial rate of pore water pressure will increase with an increase in the confining pressure.

Fig. 3 shows the variations of pore water pressure with stress under different confining pressures. The trends of 6 curves are the same and the confining pressures exhibit little effect on the relationship between pore water pressure and stress. For different confining pressures, the pore water pressure and the stress experience different maximums. As can be seen from the length of the curves, the greater the confining pressure, the longer the curve, that is the greater the maximums of the pore water pressure and the dynamic stress.

4. Study on constitutive relationship

4.1. Disturbed function

Disturbed state concept (DSC) was first proposed by Desai. Its basic idea (Wu, 2002) is that the material can be regarded as a mixture

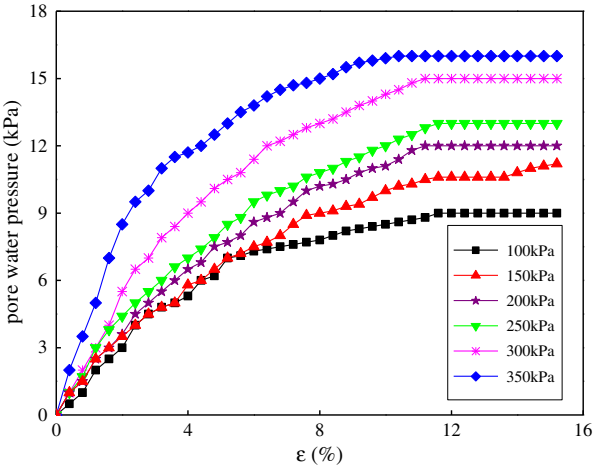

Fig. 2. Variations of pore water pressure with strain.

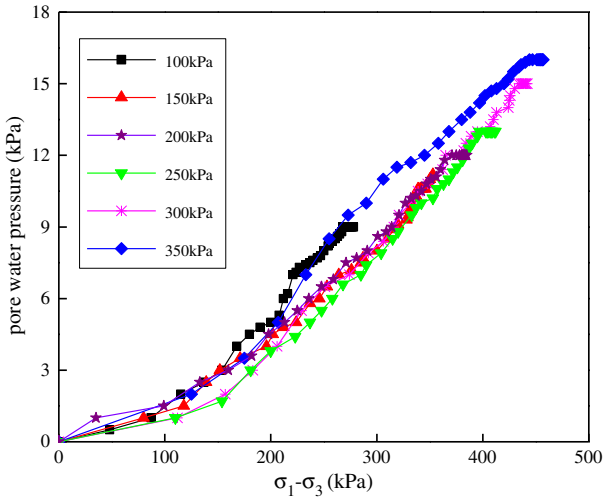

Fig. 3. Variations of the pore water pressure with stress.

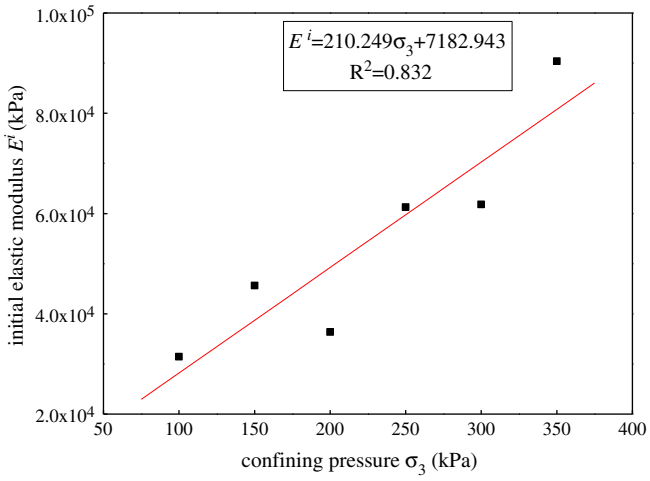

Fig. 4. Fitting curve of initial elastic modulus and confining pressure.

composed of relative intact state (RI) and fully adjusted status (FA). RI is considered as a model of linear elastic or elasto-plastic in continuum. FA denotes that the material has reached its limit state and can be simulated by critical state. The two states can be expressed by disturbed function (D). Considering the condition of the test, the problem can be simplified by the hypothesis as following: (1) The RI state of thawing soil is elastic; (2) The FA state is the limit state of failure.

Based on the effective stress principle and DSC theory, Desai and Gens (2002) defined the disturbed function as:

$$D = \frac{p_w}{p^i} \tag{1}$$

where p_w is the pore water pressure; p^i is the confining pressure.

Based on Desai's theory, Chen et al. (2004) redefined the disturbed function as:

$$D = \alpha \frac{p_w}{\sigma_3} \tag{2}$$

where α is an undetermined coefficient; σ_3 is the confining pressure.

In this paper, based on the assumptions of material and the test data, the disturbed function was defined as:

$$D = \alpha \left(\frac{p_w}{\sigma_3}\right)^{\beta} \tag{3}$$

where β is an undetermined coefficient.

Table 1
Relations of the data fitting.

σ_3(kPa)	Relation	Correlation degree	E^i(kPa)	α
100	$\frac{\sigma_1-\sigma_3}{\varepsilon} = -43308\left(\frac{p_w}{\sigma_3}\right)^{1/6} + 31457$	0.966	31,457	1.377
150	$\frac{\sigma_1-\sigma_3}{\varepsilon} = -67130\left(\frac{p_w}{\sigma_3}\right)^{1/6} + 45649$	0.952	45,649	1.471
200	$\frac{\sigma_1-\sigma_3}{\varepsilon} = -53279\left(\frac{p_w}{\sigma_3}\right)^{1/6} + 36385$	0.993	36,385	1.464
250	$\frac{\sigma_1-\sigma_3}{\varepsilon} = -96037\left(\frac{p_w}{\sigma_3}\right)^{1/6} + 61263$	0.957	61,263	1.568
300	$\frac{\sigma_1-\sigma_3}{\varepsilon} = -96328\left(\frac{p_w}{\sigma_3}\right)^{1/6} + 61805$	0.976	61,805	1.559
350	$\frac{\sigma_1-\sigma_3}{\varepsilon} = -144547\left(\frac{p_w}{\sigma_3}\right)^{1/6} + 90375$	0.987	90,375	1.599

4.2. Establishment of the constitutive relationship

In the state of fixed confining pressure, the stress–strain relationship of thawing soil can be expressed as:

$$\varepsilon = \frac{\sigma}{E^a} = \frac{\sigma}{E^i(1-D)} \tag{4}$$

where E^a and E^i are the observed elastic modulus and the initial elastic modulus, respectively. Then the constitutive relationship based on DSC can be given as:

$$\frac{\sigma_1-\sigma_3}{\varepsilon} = E^i(1-D) = E^i\left[1-\alpha\left(\frac{P_w}{\sigma_3}\right)^{\beta}\right] \tag{5}$$

The initial elastic modulus is related to the confining pressure. This paper assumes that they have linear relationship, namely

$$E^i = A\sigma_3 + Bp_a \tag{6}$$

where A and B denote undetermined coefficients; p_a is the standard atmosphere, namely, $p_a = 101$ kPa. Eq. (5) can be transformed into:

$$\frac{\sigma_1-\sigma_3}{\varepsilon} = (A\sigma_3 + Bp_w)\left[1-\alpha\left(\frac{P_w}{\sigma_3}\right)^{\beta}\right] \tag{7}$$

Eq. (7) is the constitutive relationship of thawing soil based on DSC.

According to Eq. (7), the variables are $\frac{\sigma_1-\sigma_3}{\varepsilon}$ and $\left(\frac{P_w}{\sigma_3}\right)^{\beta}$, showing linear relationship between them. Because the undetermined parameters are a lot, β can be obtained according to the correlation of the data fitting later. The correlation reaches the maximum when $\beta = \frac{1}{6}$.

In actual analysis, the stress, the strain, and the pore water pressure need to be measured under different confining pressures. E^i and α with different confining pressures can be obtained by the linear fitting between $\frac{\sigma_1-\sigma_3}{\varepsilon}$ and $\left(\frac{P_w}{\sigma_3}\right)^{1/6}$. According to Eq. (6), to the range of α, A, and B can be obtained by another linear fitting. If the data are just measured under the same confining pressure, only the linear fitting between $\frac{\sigma_1-\sigma_3}{\varepsilon}$ and $\left(\frac{P_w}{\sigma_3}\right)^{1/6}$ should be conducted. Once the constitutive relationship is obtained, the elastic modulus at any time can be calculated easily as long as the pore water pressure has been measured at the same time.

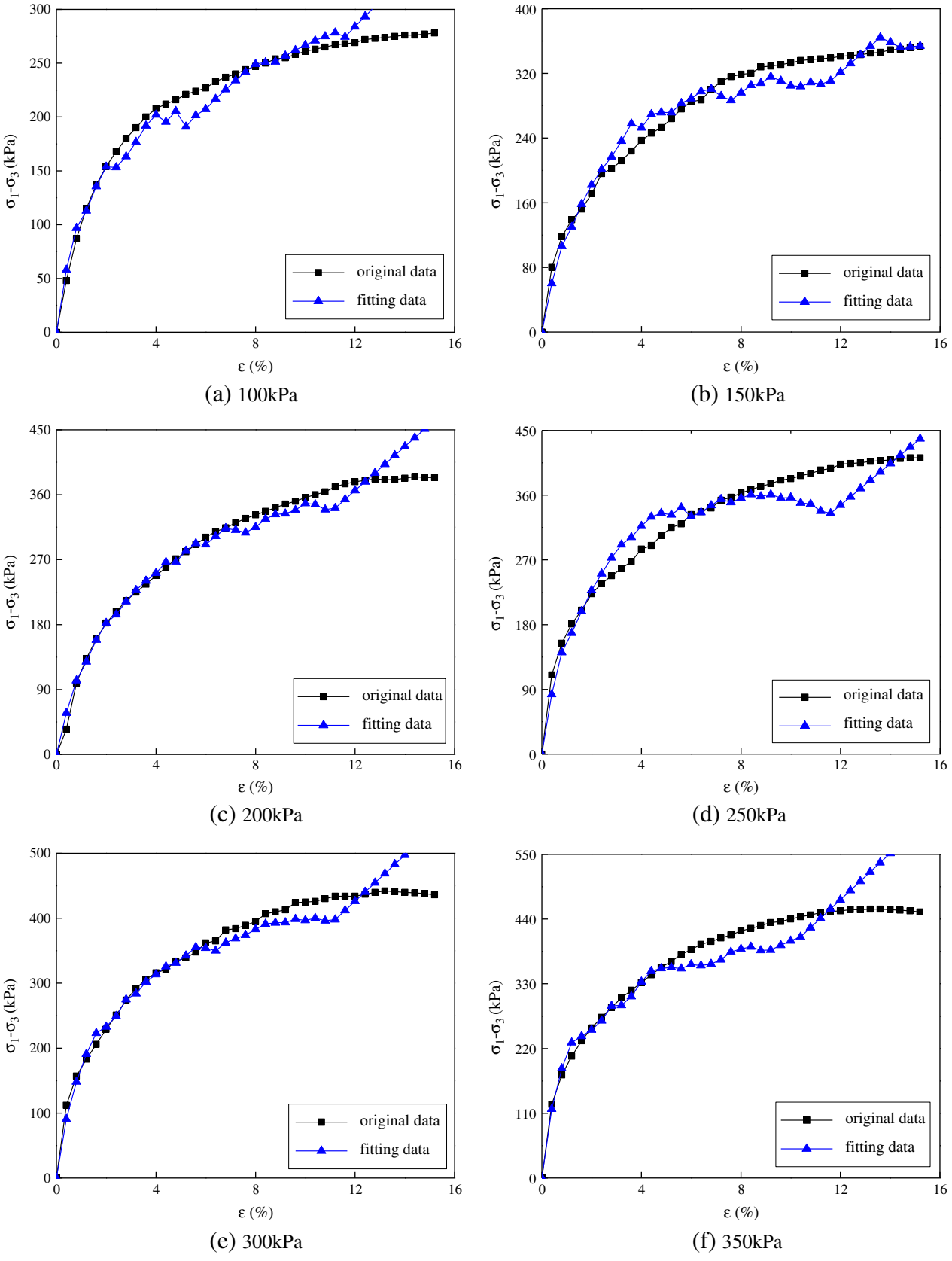

Fig. 5. Comparisons of stress–strain of the original data with that of the fitting data.

Above all, the relations between $\frac{\sigma_1-\sigma_3}{\varepsilon}$ and $\left(\frac{P_w}{\sigma_3}\right)^{1/6}$ under different confining pressures can be provided according to the fitting of test data. As shown in Table 1, $\frac{\sigma_1-\sigma_3}{\varepsilon}$ and $\left(\frac{P_w}{\sigma_3}\right)^{1/6}$ have a good linear relationship.

The relationship of E^i and σ_3 was obtained, as shown in Fig. 4. According to Table 1 and Eq. (1), A and B can be caculated.

According to the fitting results, A is equal to 210.249, and B is equal to 7182.943/101 = 71.118. The undetermined coefficient α can be calculated and α = 1.377–1.599.

4.3. Model validation

The comparisons between the original data and the fitting data under different confining pressures are shown in Fig. 5.

According to Fig. 5, the theoretical curves and the experimental curves present overlapping. Hence, they are in good agreement, especially when the strain is small. When the strain is large, there is a larger deviation between the theoretical curves and the experimental ones. It is mainly due to the strong non-linear characteristics of clay. In general, the theoretical and experimental curves are very consistent.

Through the analysis of test data, the constitutive relationship of thawing soil based on DSC can well describe the mechanical response. Due to the plastic deformation in the course of experiment, the constitutive relationship will present nonlinearity, so it will be more accurate if non-linear analysis is used. Thus this problem still needs further study.

5. Analysis of dynamic triaxial test

The data measured in the test are dynamic stress σ_d and dynamic strain ε_d, and the dynamic elastic modulus E_d can be calculated by $E_d = \frac{\sigma_d}{\varepsilon_d}$.

Figs. 6 and 7 show the σ_d–ε_d curves and the E_d–ε_d curves at different frequencies, respectively.

According to Figs. 6 and 7, the dynamic elastic modulus E_d decreases with increase in the dynamic strain ε_d. Thus, the soil strength decreases gradually with the increase of vibration times. As the three frequencies of vibration load are low, the differences of the three curves are relatively small. The curves of dynamic stress versus dynamic strain at different frequencies are fitting for hyperbola curve; therefore, Hardin–Drnevich's hyperbolic model (the equivalent linear model) can be chosen to describe the constitutive relationship (Hardin and Drnevich, 1972). The model can be expressed as:

$$\sigma_d = \frac{\varepsilon_d}{a + b\varepsilon_d} \tag{8}$$

where a and b are two constants determined by test.

Eq. (8) can be transformed as:

$$E_d = \frac{\sigma_d}{\varepsilon_d} = \frac{1}{a + b\varepsilon_d} \tag{9}$$

That is:

$$\frac{1}{E_d} = a + b\varepsilon_d \tag{10}$$

when $\varepsilon_d \to 0$, then $E_d \to \frac{1}{a}$, so $\frac{1}{a}$ denotes the initial elastic modulus $E_{d\max}$; when $\varepsilon_d \to \infty$, then $\sigma_d \to \frac{1}{b}$, thus $\frac{1}{b}$ means the maximum dynamic stress $E_{d\max}$, namely, the asymptote of the curve.

According to Eq. (10), $\frac{1}{E_d}$ and ε_d have a linear relation, therefore, the constants, a and b, can be obtained by regression analysis of a group of test data.

6. Dynamic constitutive relationship

Due to the linear relationship between $\frac{1}{E_d}$ and ε_d, Fig. 8 shows the results of fitting.

The values of $E_{d\max}$ and $\sigma_{d\max}$ can be obtained by $E_{d\max} = \frac{1}{a}$ and $\sigma_{d\max} = \frac{1}{b}$. The Poisson's ratio is equal to 0.46 from the experiment. According to the equation as follows:

$$G_{d\max} = \frac{E_{d\max}}{2(1+\mu)} \tag{11}$$

the value of $G_{d\max}$ can be given. The parameters under exciting forces of different frequencies are summarized in Table 2.

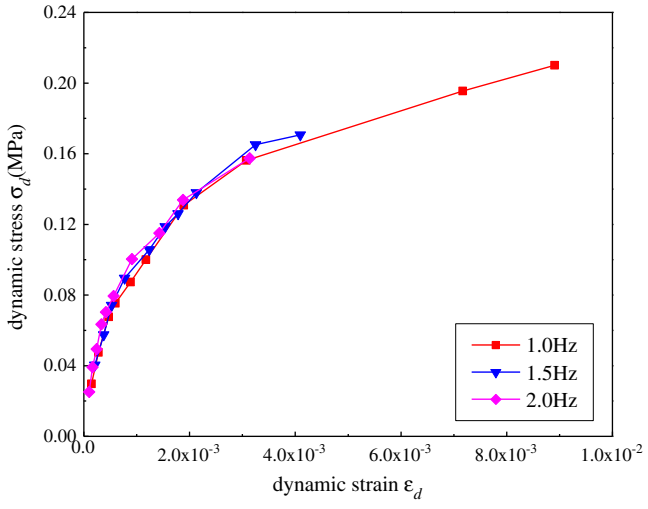

Fig. 6. Variations of dynamic stress with strain.

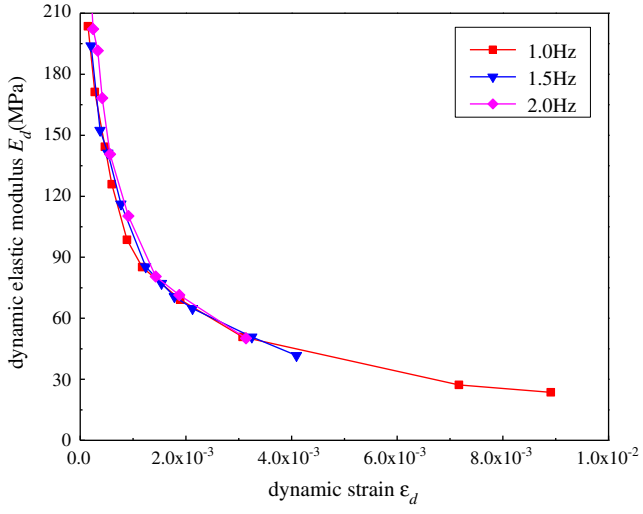

Fig. 7. Variations of dynamic elastic modulus with strain.

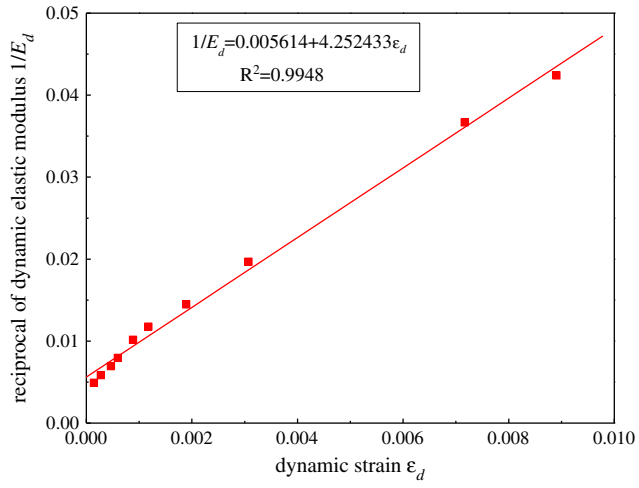

(a) 0.5Hz

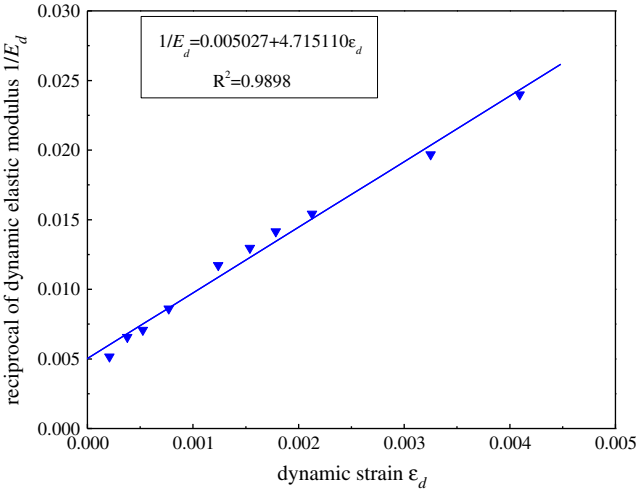

(b) 1.0Hz

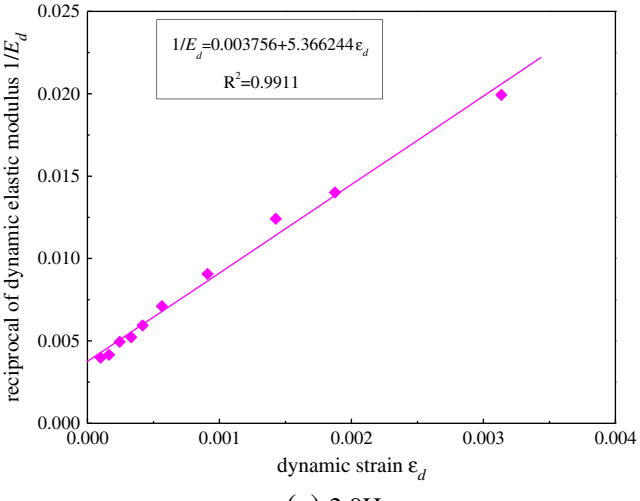

(c) 2.0Hz

Fig. 8. Fitting curves of $\frac{1}{E_d}$ and ε_d.

For the sake of comparisons of thawing soil and undisturbed soil, the dynamic test of the undisturbed soil was conducted under the same conditions as that of thawing soil. The parameters are summarized in Table 3.

Table 2
Mechanical parameters of thawing soil at different frequencies.

Frequencies of vibration loads f(Hz)	E_{dmax}(Mpa)	σ_{dmax}(Mpa)	G_{dmax}(Mpa)
1.0	178.13	23.52	61.00
1.5	198.93	21.21	68.13
2.0	266.24	18.74	91.18

Table 3
Mechanical parameters of undisturbed soil at different frequencies.

Frequencies of vibration loads f(Hz)	E_{dmax}(Mpa)	σ_{dmax}(Mpa)	G_{dmax}(Mpa)
1.0	196.07	20.45	67.61
1.5	212.77	17.36	73.36
2.0	263.16	10.04	90.74

Comparisons between Tables 2 and 3 indicate that the maximum dynamic stress σ_{dmax} increases after freezing and thawing. The increases are as follows:

when $f = 1.0$Hz, the increasing amount of the maximum dynamic stress $\Delta\sigma_{max} = 3.07$ Mpa, $\Delta\sigma_{max} / \sigma_{max} = 15.01\%$;
when $f = 1.5$Hz, the increasing amount of the maximum dynamic stress $\Delta\sigma_{max} = 3.85$ Mpa, $\Delta\sigma_{max} / \sigma_{max} = 22.18\%$;
when $f = 2.0$Hz, the increasing amount of the maximum dynamic stress $\Delta\sigma_{max} = 8.70$ Mpa, $\Delta\sigma_{max} / \sigma_{max} = 86.65\%$;

According to Fig. 9, the maximum dynamic stress increases exponentially with frequency. It is mainly due to that the pore water in soil is frozen in the process of freezing. The volume expansion of soil destroys the soil structure, and the gaps caused by expansion will be filled, frozen and destructed by the surrounding pore water which is unfrozen again. The physical and mechanical properties of soil will deteriorate after several cycles of freezing and thawing, and its bearing capacity will reduce at the same time.

7. Analysis of microstructure

7.1. Quantitative analysis of microscopic parameters

The SEM images before and after freezing and thawing were processed and the quantitative parameters used for describing the microstructure were extracted. In order to describe the microstructure better, four representative parameters (Equivalent diameter D_E, Eccentricity e, Directional frequency F and fractal dimension of pore morphology D) were selected.

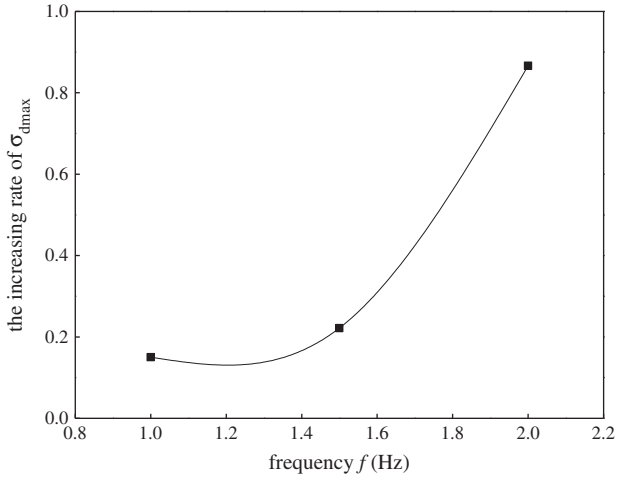

Fig. 9. Variations of dynamic stress with frequency.

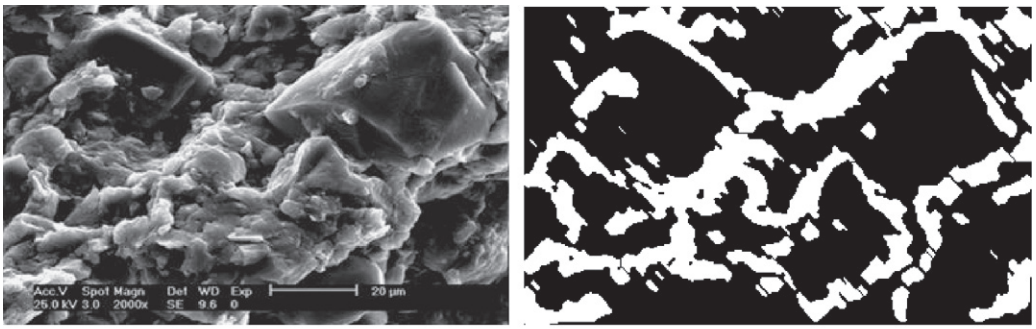

(a) Before freezing and thawing

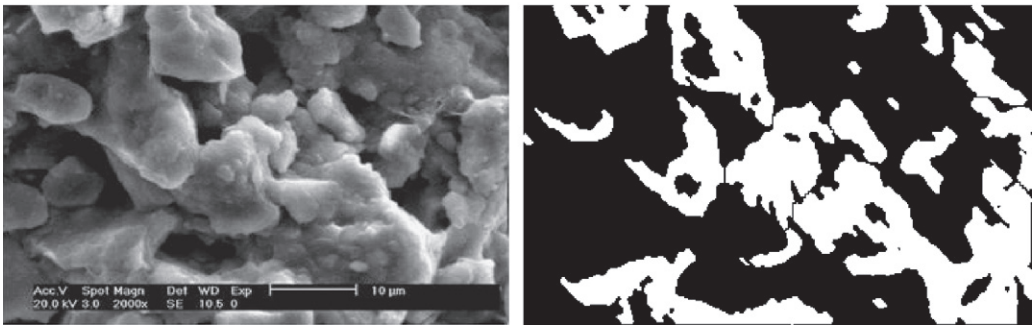

(b) After freezing and thawing

Fig. 10. SEM images and binary images.

Fig. 10 shows the SEM images and binary images processed by matlab with the threshold of 0.35.

The equivalent diameter D_E and eccentricity e of each pore were extracted with matlab from the binary images. The averages of equivalent diameter and eccentricity are summarized in Table 4.

According to Table 4, the equivalent diameters of thawing soil reduce, and the main reason is that the cementation body between soil particles was damaged in the process when the pore water were frozen to ice, causing disintegration and dispersion of the soil particles to some extent. If the soil just underwent the process of freezing and thawing but no consolidation, the changes of eccentricity are relatively small.

The range of pore orientation angles extracted by matlab is [−90°, 90°], in order to transform the range to [0°, 180°], the data less than 0° were added 180°. Moreover, for the sake of the integrity of statistical regularities, the data within the range of [0°, 180°] above were also added 180°, and all the data were plotted on the same graph. According to the above rules of transformation, the graph should be centrosymmetric. Fig. 11 presents the distribution of pore orientation angles before and after freezing and thawing. The graphs are centrosymmetric as expected. According to the analysis and comparison between Fig. 11(a) and (b), the distributions of pore orientation angles before and after freezing and thawing are quite uneven, showing strong directionality. However, due to the damage of structural in the course of freezing and thawing, the distribution of pore orientation angles after freezing and thawing exhibits greater randomness than that of undisturbed soil.

Table 4
Parameters of pore before and after freezing and thawing.

Pore parameter	Before freezing and thawing	After freezing and thawing
Average of equivalent diameters $\overline{D_E}$ (μm)	5.8225	5.4303
Average of eccentricities $\overline{e}$	0.8671	0.8600

In general, the pore of soil has fractal characteristics. The relationship between the equivalent perimeter and the area can be expressed as:

$$\log_{10}(p) = \frac{D}{2} \times \log_{10}(A) + C \tag{12}$$

where p denotes the equivalent perimeter; A is the area of pore; D is the fractal dimension of pore; C is a constant.

According to Eq. (12), provided that the values of equivalent perimeters and areas are drawn and fitted in the double logarithmic coordinates, the fractal dimension of pore should be twice of the slope of fitting line. Fig. 12 shows the fitting curves.

According to Fig. 12, the fractal dimension reduces after freezing and thawing, showing that the pore morphology before freezing and thawing is more complex than that after freezing and thawing. The amplitude reduction is just 1.43%, indicating that the freezing and thawing action changes fractal dimension little.

7.2. Relationship between macroscopic phenomena and microstructure

After freezing and thawing, the pore characteristics of soil will change, and the changes will inevitably lead to the changes of soil skeleton characteristic. The SEM images depict that the freeze of pore water makes parts of the origin small pores closed. This will cause the contacts of soil particles decrease, and it is not conducive to the friction between soil particles. The cohesion in the soil mainly depends on the cementation force and occlusion between soil particles etc. The damage of soil structure during the freezing and thawing decreases the cementation force. Therefore, the cohesion will reduce, leading to the decrease of shear strength and bearing capacity of soil. So the mechanical characteristics of thawing soil are worse than those of undisturbed soil.

8. Conclusions

This paper studied the physical parameters of soil and given the constitutive equation under static load. Based on the dynamic triaxial test, the dynamic characteristics of thawing soil and undisturbed soil were

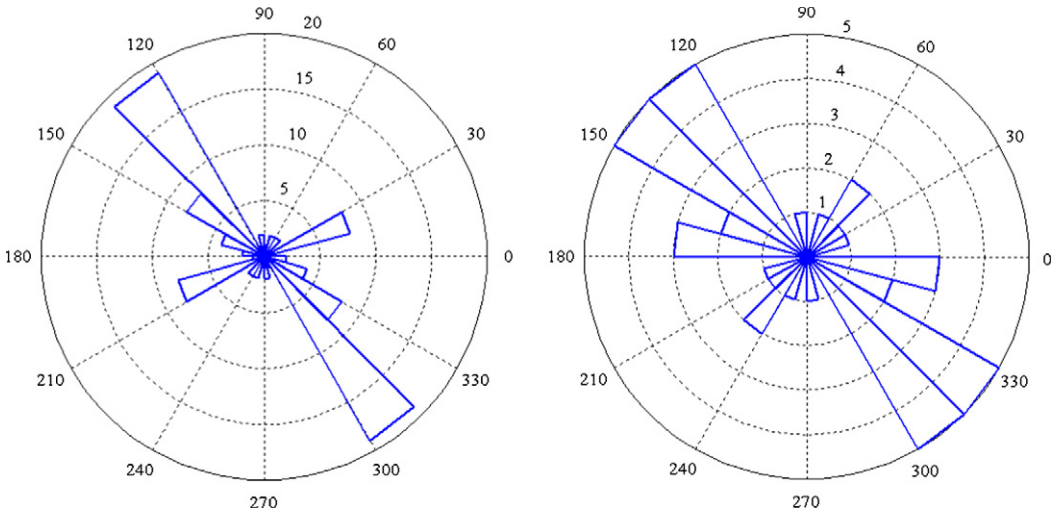

(a) Before freezing and thawing (b) After freezing and thawing

Fig. 11. Distribution of pore orientation angles.

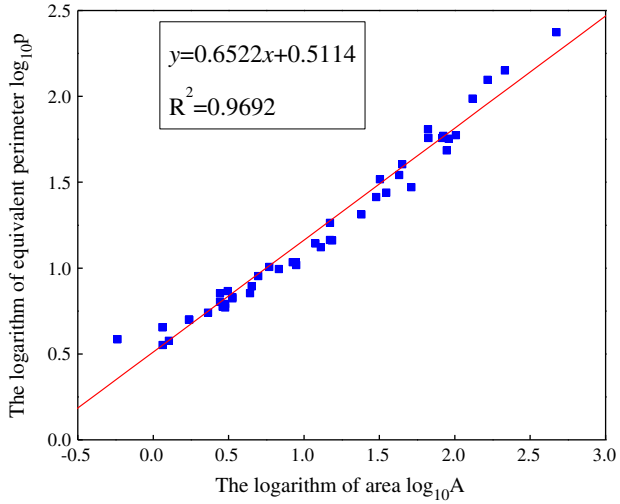

(a) Before freezing and thawing ($D = 2k = 1.3044$)

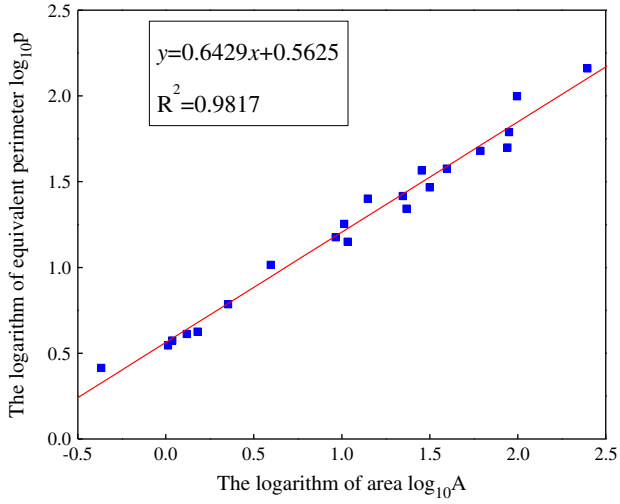

(b) After freezing and thawing ($D = 2k = 1.2858$)

Fig. 12. Fitting curves of the equivalent perimeters and the areas.

analyzed and compared. The dynamic constitutive relationship was obtained. The microscopic parameters were obtained by the process of SEM images before and after freezing and thawing, and the changes were analyzed from micro perspective.

(1) The increment rate of strain decreases with an increase in the stress. The dynamic stress tends to be constant. The dynamic stress–strain curve is fitting for hyperbola curve, so is the relationship of pore water pressure versus dynamic strain. The stable values of pore water pressure and stress increase with an increase in the confining pressure.
(2) According to the results of static triaxial test, the disturbed function was given and the constitutive relationship of thawing soil was obtained.
(3) The dynamic elastic modulus E_d decreases with an increase in the dynamic strain ε_d. The maximum dynamic stress increases after freezing and thawing based on the comparison between thawing soil and undisturbed soil.
(4) After freezing and thawing, the soil becomes looser and the equivalent diameter decreases; the distributions of pore orientation angles before and after freezing and thawing show strong directionality, but it appears a certain degree of reduction after freezing and thawing; the freezing and thawing has little influence on the eccentricity and fractal dimension of pores.

Acknowledgements

This work presented in this paper was supported by the National Natural Science Foundation of China (Grant No. 51208503) and the Natural Science Foundation of Jiangsu Province, China (Grant No. BK2012133).

References

Bondarenko, G., Sadovsky, A., 1991. Water content effect of the thawing clay soils on shear strength. Proceedings of 7th International Symposium on Ground Freezing. A. A. Balkema, Rotterdam, Netherlands, pp. 123–127.
Brams, B., Yao, L., 1964. Shear strength of a soil after freezing and thawing. ASCE J. Soil Mech. Found. Div. 90, 1–26.
Chen, J., Wu, G., Wang, J., Hao, J., 2004. The mechanical properties of saturated soft clay based on the disturbed state concept. J. Xi'an Shanghai Univ. 38, 952–955.
Cui, Z., Tang, Y., 2011. Microstructures of different soil layers caused by the high-rise building group in Shanghai. Environ. Earth Sci. 63, 109–119.
Delage, P., Audiguier, M., Cui, Y., Howatt, M., 1996. Microstructure of a compacted silt. Can. Geotech. 33, 150–158.

Desai, C., Gens, A., 2002. Mechanics of Materials and Interfaces: the Disturbed State Concept. CRC press.
Elliott, R., Thornton, S., 1988. Resilient modulus and aashto pavement design. Transp. Res. Rec. 1196, 116–124.
Graham, J., Au, V., 1985. Effects of freeze–thaw and softening on a natural clay at low stresses. Can. Geotech. J. 22, 69–78.
Hardin, B., Drnevich, V., 1972. Shear modulus and damping in soils: design equations and curves. Journal of the Soil Mechanics and Foundation Division, ASCE 98, 667–692.
Inozemtsev, V., 1986. Effect of dynamic action on compressibility of thawing sands. Soil Mech. Found. Eng. 23, 235–240.
Konrad, J., 1989. Physical processes during freeze–thaw cycles in clayey silts. Cold Reg. Sci. Technol. 16, 291–303.
Lai, Y., Wu, Z., Zhu, Y., et al., 1999. Nonlinear analysis for the coupled problem of temperature and seepage fields in cold region tunnels. Cold Reg. Sci. Technol. 29, 89–96.
Lai, Y., Wu, Z., Zhu, Y., et al., 2000. Elastic visco-plastic analysis for earthquake response of tunnels in cold regions. Cold Reg. Sci. Technol. 31, 175–188.
Lai, Y., Xu, X., Dong, Y., et al., 2013. Present situation and prospect of mechanical research on frozen soils in China. Cold Reg. Sci. Technol. 87, 6–18.
Leroueil, S., Tardif, J., Roy, M., et al., 1991. Effects of frost on the mechanical behavior of Champlain Sea clays. Can. Geotech. J. 28, 690–697.
Li, Q., Ling, X., Wang, L., et al., 2013. Accumulative strain of clays in cold region under long-term low-level repeated cyclic loading: experimental evidence and accumulation model. Cold Reg. Sci. Technol. 94, 45–52.
Ling, X., Zh, Z., Wang, L., et al., 2009. Dynamic elastic modulus for frozen soil from the embankment on Beiluhe Basin along Qinghai–Tibet Railway. Cold Reg. Sci. Technol. 57, 7–12.
Ling, X., Li, Q., Wang, L., et al., 2013. Stiffness and damping radio evolution of frozen clays under long.term low.level repeated cyclic loading: Experimental evidence and evolution model. Cold Reg. Sci. Technol. 86, 45–54.
Liu, J., Peng, L., 2009. Experimental study on the unconfined compression of a thawing soil. Cold Reg. Sci. Technol. 58, 92–96.
Mahmoud, G., Mahya, R., 2013. Freeze–thaw performance of clayey soil reinforced with geotextile layer. Cold Reg. Sci. Technol. 89, 22–29.
Murat, O., 2013. The effects and optimization of additives for expansive clays under freeze–thaw conditions. Cold Reg. Sci. Technol. 93, 36–46.
Ono, T., Mitachi, T., 1997. Computer controlled triaxial freeze thaw-shearapparatus. Proceedings of 8th International Symposium of Ground Freezing. A. A. Balkema, Rotterdam, Netherlands, pp. 335–339.
Pusch, R., Schomburg, J., 1999. Impact of microstructure on the hydraulic conductivity of undisturbed and artificially prepared smectite clay. Eng. Geol. 54, 167–172.
Qi, J., Vermeer, P., Cheng, G., 2006. A review of the influence of freeze–thaw cycles on soil geotechnical properties. Permafr. Periglac. Process. 17, 245–252.
Qi, J., Ma, W., Song, C., 2008. Influence of freeze–thaw on engineering properties of a silty soil. Cold Reg. Sci. Technol. 53, 397–404.
Simonsen, E., Isacsson, U., 2001. Soil behavior during freezing and thawing using variable and constant confining pressure triaxial tests. Can. Geotech. J. 38, 863–875.
Simonsen, E., Janoo, V., Isacsson, U., 2002. Resilient properties of unbound road materials during seasonal frost conditions. J. Cold Reg. Eng. 16, 28–50.
Wu, G., 2002. The constitutive model of engineering materials in the disturbed state-disturbed state concept and its theoretical basis. Chin. J. Rock Mech. Eng. 21, 759–765.
Yong, R., Boonsinsuk, P., Yin, C., 1985. Alternation of soil behaviour after cyclic freezing and thawing. Proceedings of 4th International Symposium on Ground Freezing. A. A. Balkema, Rotterdam, the Netherlands, pp. 187–195.
Zhang, H., Feng, K., 1993. Mechanism of the attenuation of strength for loess-cement under cyclical freezing and thawing. J. Glaciol. Geocryol. 1, 175–181.